A comparison of track model formulations for simulation of dynamic vehicle–track interaction in switches and crossings

(article starts on next page)

Taylor & Francis
Taylor & Francis Group

A comparison of track model formulations for simulation of dynamic vehicle–track interaction in switches and crossings

Björn A. Pålsson, Ramakrishnan Ambur, Michel Sebès, Ping Wang, Jou-Yi Shih, Demeng Fan, Jingmang Xu & Jiayin Chen

Published online: 19 Oct 2021.

Submit your article to this journal ☑

Article views: 158

View related articles ☑

View Crossmark data ☑

🔓 OPEN ACCESS Check for updates

A comparison of track model formulations for simulation of dynamic vehicle–track interaction in switches and crossings

Björn A. Pålsson [a], Ramakrishnan Ambur [b], Michel Sebès[d], Ping Wang [f], Jou-Yi Shih [b,c], Demeng Fan[d,e], Jingmang Xu[f] and Jiayin Chen [f]

aDepartment of Mechanics and Maritime Sciences/CHARMEC, Chalmers University of Technology, Göteborg, Sweden; bBirmingham Centre for Railway Research and Education, University of Birmingham, Birmingham, UK; cZynaMic Engineering, Stockholm, Sweden; dCOSYS, Univ. Gustave Eiffel, IFSTTAR, Marne la Vallée, France; eESI Group, Paris, France; fKey Laboratory of High-Speed Railway Engineering, Ministry of Education, Southwest Jiaotong University, Chengdu, People's Republic of China

ABSTRACT

This paper compares different track model formulations for the simulation of dynamic vehicle–track interaction in switches and crossings (S&C, turnouts) in a multi-body simulation (MBS) environment. The investigations are an extension of the S&C simulation Benchmark with the addition of a finite element model of a 60E1-760-1:15 turnout. This model constitutes a common reference from which four different track formulations are derived: co-running, modal superposition, finite element incorporated into the MBS model and finite element coupled to MBS using a co-simulation approach. For the different track models, the difference in modelling technique, results, simulation time, and suitability for different simulation tasks is compared. A good agreement is found between the different track model formulations for wheel–rail contact forces and rail displacements. This study found a better agreement between co-running and structural track models compared to previous studies in the prediction of wheel–rail contact forces. This appears to be due to the increased complexity of co-running track model used in this study together with a tuning of the co-running track model to the reference model in a wider frequency range. For the reader interested to reproduce the results in this paper, the reference track model is available for download.

Introduction

This paper compares different track model formulations for simulation of dynamic vehicle-track interaction in switches and crossings (S&C, turnout) in a multi-body simulation (MBS) environment. The investigation is an extension of the S&C simulation Benchmark [1,2] with the addition of a finite element (FE) model of a 60E1-760-1:15 turnout [3]. This model constitutes a common reference from which the different track model formulations are derived. The participating institutions and their software and track formulations are listed in Table 1. A co-running track model, as used by UoB, is a representation of the

---

CONTACT Björn A. Pålsson ✉ bjorn.palsson@chalmers.se

Table 1. Track model formulations and software in the present study.

Partner	Plot abbreviation	Track model type	Software
University of Birmingham/ZynaMic Engineering AB	UoB	Co-running	Simpack 2018x.2
Southwest Jiaotong University	SWJTU	Finite element	SDITT [11]
ESI Group/Univ Gustave Eiffel/IFSTTAR	Univ. Eiffel	Finite element in co-simulation	VOCO 2020
Chalmers University of Technology	Chalmers	Modal superposition	Simpack 2021.2

track flexibility that is positioned under each wheelset and moves along the track with the vehicle in simulation. It is typically built from a planar system of rigid bodies connected by bushing elements that form a cross-section of the track [4,5]. The FE track models use a full FE discretisation of a discretely supported track where beam elements are used to model rails and sleepers and bushing elements are used to represent rail pads and ballast [6,7]. The FE model is either incorporated in the multi-body software (SWJTU) or coupled to the MBS code using a co-simulation scheme (Univ. Eiffel). In co-simulation the coupled vehicle-track interaction problem is solved in a distributed manner where vehicle and track are modelled in different software but are coupled together in time-domain simulations by exchanging responses at the wheel–rail interface [8]. In the modal superposition approach, as used by Chalmers, the track flexibility is represented by normal modes [9,10] derived from the reference finite element model. Unless otherwise noted, the track model is the only change made to the simulation model of each partner from their original Benchmark contribution. The present track models cover most of the common choices in MBS time-domain simulations.

For the different track models, the difference in modelling technique, results, simulation time, and suitability for different simulation tasks is compared. In addition, the influence from the modal cut-off frequency on the dynamic wheel–rail contact force during the crossing transition is investigated for the modal superposition track model. Additional modelling aspects are covered in parallel papers [12–14]. It can be noted that different software is used to compare different track modelling techniques which naturally adds a confounding element. On the other hand, all software demonstrates a good base-line agreement in the S&C Benchmark, and it is apparent that the underlying properties of the different modelling techniques surface in the comparisons.

For the reader interested to reproduce the results in this paper, the reference track model is available for download [3]. The remaining input data required to model and simulate the cases presented in this paper is available from the S&C Benchmark definition [2].

Related work on track modelling

While there are comprehensive surveys available on track modelling, e.g. [5] and Chapter 6 of [15], they are focused on the modelling of plain line, i.e. standard railway track that is uniform and continuous without any S&C. While the same form of track structure and modelling techniques are applicable for S&C, they constitute a separate track modelling challenge. Because of the varying track and rail sections throughout S&C, track properties will vary along the track by design and wheels passing through a switch or a crossing panel can make simultaneous contact with multiple rail bodies that can deform relative to one-another, i.e. the stock rail and switch rail in the switch panel and the check rail and stock rail in the crossing panel.

These aspects call for more elaborate track modelling compared to plain line. These properties also make the use of modelling techniques that rely on a periodic structure, sometimes used for plain line, infeasible. S&C instead feature two discrete wheel transition areas over a limited distance. This means that more detailed structural modelling is called for in S&C, but also that it is more feasible given the limited track distance covered.

Even though there is a lack of track modelling surveys for S&C, there are papers that compare different track model formulations. Kassa and Nielsen compare a 7 degrees of freedom (dof) co-running track model in MBS software Gensys and a modal superposition structural track model with up to 500 modes in DIFF3D in [10]. Good agreement in wheel–rail contact forces is obtained for the lower frequency content, while discrepancies are observed in the rail transition areas in the switch and crossing panels. Two different structural turnout models are compared to one another and measured accelerations in [16]. The first model uses a simplified finite element model for the turnout. The second focus on the details of the turnout, which is modelled with three-dimensional finite elements. As the traffic was modelled in different ways (MBS vs. simplified vertical wheel–rail dynamics) the influence of the track model was not isolated, but good agreement was found between the models and measured accelerations.

In [17] Jorge et al. compares three different track models for the simulation of dynamic vehicle-turnout interaction, one co-running track model and two different discretely supported track models. For the models with discrete supports, one represented a single lane track while the other accounted for a double track in a cross-over assembly. The models showed good agreement for the lower frequency interaction in the switch panel while the discrepancy was large for the dynamic impact load at the crossing. It was also shown that tuning the co-running track to the properties of one of the discretely supported tracks at lower frequencies reduced the discrepancy significantly. It is stated that a better match is expected if the tuning is performed in a wider frequency range. Wan et al. [18] focus on the VI-Rail software, and compared a co-running track model to a flexible track model whose rails were modelled as FE beams and that represented the varying track stiffness along the length of the S&C. The comparison indicates that their normal contact pressures and forces are in good agreement after low-pass filtering with cut-off frequency 500 Hz. Related investigations into different track formulations for plain line are for example found in [19–21].

The present paper aims to extend the knowledge gained from these papers for the application to S&C by including additional software and model formulations as well as providing a reference turnout model for future studies.

Common finite element turnout model

To allow for a direct comparison between the different track model formulations, a common finite element (FE) track model of a 60E1-760-1:15 turnout is used as a starting point (60E1 rail, 760 m radius and 1:15 turnout angle). The model is a two-layer track model [5] with rails and sleepers modelled using linear Timoshenko beam elements while rail pads and ballast are modelled using discrete Kelvin bushing elements with stiffness and viscous damping. A layout plan of the model is presented in Figure 1. To allow for simulated train passages to start before the turnout, plain line track extensions with the same track type
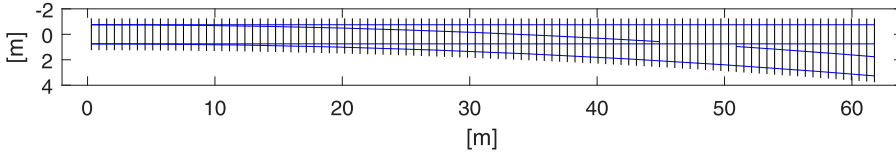
Figure 1. Layout of 60E1-760-1:15 common turnout FE model.

are used to allow for simulations to be initialised with the vehicle in front of the turnout. The overall length of the model is 62 m without track extension.

The model is linear and can be represented using an equation system on the form

$$M\ddot{u} + C\dot{u} + Ku = f \tag{1}$$

Where M, C, and K are the mass, viscous damping and stiffness matrix, respectively. u is the nodal displacement field and f the applied nodal force vector.

In terms of the track behaviour that the model should represent, lower frequency wheel–rail interaction and the relative flexibility between the stock and switch rails is of greatest interest in the switch panel while higher frequency vertical wheel–rail interaction is of greatest interest in the crossing panel [22]. The intention is that the model should capture vertical wheel–rail interaction phenomena up to about 1 kHz at the crossing transition. Around this frequency is the pinned-pinned resonance where the wavelength of the bending waves is twice that of the sleeper spacing (chapter 6 of [15]). This is a lightly damped mode where the rails displace on the sleeper spans but are stationary above the sleepers describing a standing wave mode shape. Around 1 kHz is also the so-called P_1 impact force that can be observed during wheel impacts in crossings and dipped joints that result in the wheel oscillating out-of-phase with the rail [23]. To provide margin to the frequency range of interest, the rail discretisation with four elements per sleeper span can capture mode forms up to about 2 kHz. According to [5], the single Timoshenko beam elements used are sufficient to capture vertical rail dynamics up to 2.5 kHz. For lateral and bending modes in the rails the modelling should be sufficient to capture phenomena up to 500 Hz. These numbers apply to standard rails. A crossing rail has a different construction but is assumed to have the same bending stiffness to weight ratio as a standard rail. It is also assumed that two-noded beam elements with uniform properties can represent the crossing behaviour in similar frequency ranges, especially in the vertical direction that is of greatest interest at the crossing transition.

In this study, the rail nodes are constrained such that they cannot move longitudinally nor rotate about the longitudinal axis. The rail nodes are thus free to displace laterally and vertically, but rail roll is not accounted for. The sleeper nodes are free to displace in the vertical plane through each sleeper but constrained otherwise. Full details on the model properties and discretisation are given in the Appendix. The model is also available for download [3]. It is provided as an input deck for the commercial FE software Abaqus. The bushing properties and nodal constraints in the model are parameterised via a Matlab script.

Track model variations

In the following sections, it is presented how each participant implemented their track model formulation from the common FE model.
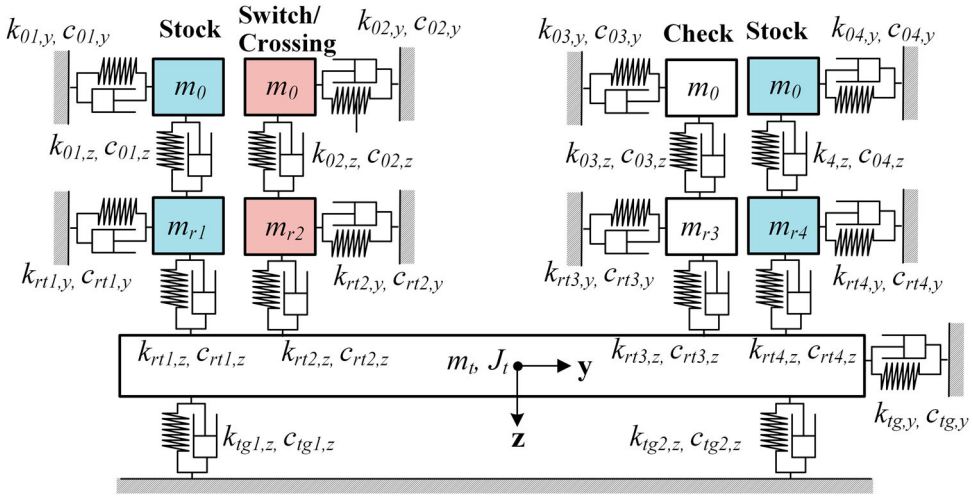
Figure 2. Three-layered co-running track model with 19 dofs [24].

Co-running track model with space-dependent parameters (UoB)

This track model entry concerns a co-running track model with space dependent parameters. The three-layered model with additional bodies and degrees of freedom compared to the S&C Benchmark model is presented in Figure 2. The additional degrees of freedom increase the rail receptance amplitude at higher frequencies. The three-layered co-running track model has shown better agreement with the present S&C FE model at higher frequencies compared to a two-layered track model and is recommended to be used for vehicle-S&C interaction dynamics in the crossing region, especially for higher train speeds (e.g. Run #7 of the benchmark [2]).

The co-running track model has been implemented in Simpack with space-dependent masses, springs and dampers tuned from the common FE model. The method for calculating the equivalent co-running track parameters for the turnout are inspired by [20,21], which takes into account the track's effective length from an infinite beam on elastic foundation. The parameters are derived based on the given track parameters and the calculated static track stiffness along the common FE model.

The simulation is split into three different track zones due to limitations of the software which does not allow for the masses to vary during simulation. Therefore, each simulation zone has constant mass values and the masses are changed before re-starting the next simulation zone. This is naturally an approximation as for example the switch rail gradually increases in mass from the switch toe. The first zone starts just before the switch toe and extends until the crossing. The second zone covers the crossing region and the third zone covers a small portion of plain track after the crossing region. The stiffness and damping properties of various elements were defined as continuous functions throughout the turnout. To prevent this discontinuity from affecting the results in a region of interest such as the transition zone, the simulation zone breaks are positioned a distance before the regions of interest. A detailed description of the methodology can be found in [24].

Co-simulation between finite elements and VOCO (Univ-Eiffel)

This track model entry concerns Co-simulation using FE code Ansys and MBS code VOCO. The Co-simulation methodology has been used in a preceding study [25] and its principle and implementation is presented below. The co-simulation is non-intrusive and could be performed with other FE solvers than Ansys. It uses the same coupling scheme as VOCO's own track models. A comparable co-simulation procedure has also been used with other MBS packages [26].

Principle of the co-simulation

In the co-simulation scheme, the vehicle-track interaction problem is split into two sub-problems: vehicle dynamics is carried out in VOCO, and track dynamics is computed in Ansys. Non-linear features may be activated in the FE model. Both problems are solved alternatively with a common time step and are coupled in a co-simulation logic. Wheel/rail (w/r) contact forces are computed in the vehicle block and are then transmitted to the track block. Coupling is realised by a feedback of the structural track displacements into the vehicle block. The track dynamics is governed by Equation (1), where f is the vector of w/r forces projected on the u basis. This projection is carried out by distributing w/r forces on FE rail nodes adjacent to the wheel position with Hermitian cubic shape functions [25]. The vector of rail displacements under each wheel u_r is deduced from the u dofs using the same shape functions. The vehicle dynamics is governed by Equation (2):

$$M_v \ddot{u}_v + C_v \dot{u}_v + K_v u_v = f_c \qquad (2)$$

where M_v, C_v and K_v are respectively the mass, damping and stiffness matrices of the vehicle model. u_v is the vector of vehicle dofs. f_c is the vector of w/r forces. W/r forces are functions of the wheel and rail positions and velocities. The coupling of the track and vehicle models consists in adding the structural rail displacements u_r, and their derivative with respect to time, in the expressions of the rail positions and velocities. In case a wheel makes simultaneous contact with multiple rail bodies, the expression of u_r is a weighed sum of the vertical forces acting on each body i according to Equation (3):

$$u_r = \frac{\sum Q_i u_{r,i}}{\sum Q_i} \qquad (3)$$

An improvement on the previously used procedure [25] is to consider the check rail in the coupling of the vehicle and track models. Another improvement concerns the modelling of the check rail itself as documented in the summary of the method statements [1], and the individual online method statements of VOCO [27].

In the FE model, there is no direct structural connection in the lateral direction between the switch rail and the stock rail. This approximation of the physical model may lead to some numerical instabilities when the previous expression is used in the diverging route as already mentioned in the benchmark [27]. These instabilities are due to the lateral motion of both rails being forced together by lateral forces acting in opposite directions. The model is somewhat unrealistic as both rails may intrude in each other. A workaround already used in the benchmark consists in discarding the stock rail lateral displacement in the above expression assuming that the lateral motion of the switch rail is prominent in the lateral
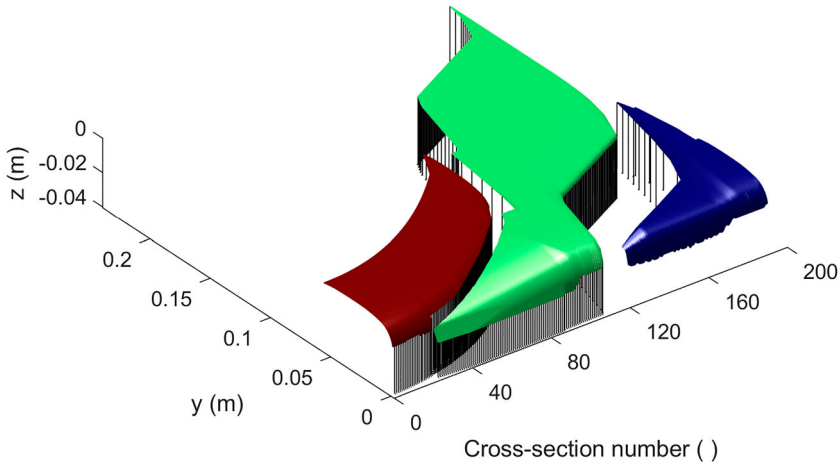
Figure 3. Compacted view of the VOCO contact model of the turnout.

direction. The influence of the separation of the stock rail and switch rail has been studied in parallell papers [12,13].

Procedure of co-simulation

Ansys release 2021 R1 [28] has been used in this study and the common track model in Abaqus format has been translated into an Ansys model. As specified in the benchmark [2], the vehicle has 25 m of running on a perfectly tangent track before it reaches the front of the turnout. Consequently, 47 m of tangent track have been added to the FE model accounting for these 25 m plus the length of the vehicle. FE model statistics are: 16,225 elements, 16,821 nodes, and 21,740 active dofs for the whole track including the extension.

A transient analysis is performed with the full solution method [28] using the default options. No additional damping is added to the FE model. Track model initial conditions are non-zero displacements due to gravity and zero velocities. Wheel loads are progressively applied on the track model during the first few metres of the simulation.

VOCO simulations are carried out with the same solver settings as in run #7 of the benchmark (60E1-760-1:15 crossing in a through route).

A compacted view of the contact model of the MBS is shown in Figure 3. The model is composed of 200 cross-sections. Each cross-section is discretised into 3 segments, each of them associated with one rail body of the S&C:

(1) Stock rail at the beginning of the turnout (red),
(2) Switch rail and wing rail (green),
(3) Crossing nose and stock rail at the end of the turnout (blue).

Each rail body segment is in turn discretised into 200 strips in the y-direction for contact calculations.

The same time step Δt is used in VOCO and Ansys. A constant 1e-5 s time step provides stable results in the through route with a computing time of 17 hours. In the diverging

route, a 0.5e-5 s time step is required in the switch panel while a 1e-5 s time step is used in the remainder of the track: computing time is then 40 h.

Simulation using SDITT (SWJTU)

This track model entry concerns a coupled MBS-FE formulation using the in-house program SDITT (Simulation of Dynamic Interaction between Train and Turnout). The FE track model in SDITT is based on the common FE model, but it has been re-discretised to reduce the computational effort. The details are as follows:

- The turnout rails are modelled using discretely supported Euler beams. All rail nodes have 4 dofs as in the common FE model as the longitudinal and roll dofs are constrained.
- To simulate the effect of variable cross-sections on the turnout rails' bending stiffness, the beam cross-sectional properties of switch rails are varied from one element to the next. To reduce the computational effort, the FE discretisation is changed compared with the common FE model. The switch rail and crossing rail are divided into 4 elements per sleeper span, while other rails are subdivided into 2 elements per sleeper span.
- The sleepers are simulated as discretely supported Euler beams in the vertical direction and rigid bodies in the lateral direction. Each sleeper is divided into 9–31 nodes according to its lateral length. In addition to the rigid lateral displacement of the sleeper, each sleeper node has 2 dofs, including the vertical and rolling deformation as in the common FE model. Rail fastening systems and ballast are modelled with linear bushing elements as in the common FE model.
- To eliminate any structural boundary effect when the vehicle enters the turnout, 25 m of extended tangent track is added in front of the turnout to create a continuous track. Considering the track extension, the turnout model contains 2668 sleeper elements, 1222 rail elements, 4042 nodes and 10,687 active dofs.

The mass matrix M_e and stiffness matrix K_e of the Euler beam element is defined in Equations (4) and (5), respectively:

$$M_e = \begin{bmatrix} 156A & 22Aa & 54A & -13Aa \\ 22Aa & 4Aa^2 & 13Aa & -3Aa^2 \\ 54A & 13Aa & 156A & -22Aa \\ -13Aa & -3Aa^2 & -22Aa & 4Aa^2 \end{bmatrix}, \quad A = m_r a/420 \qquad (4)$$

$$K_e = \begin{bmatrix} 12B & 6Ba & -12B & 6Ba \\ 6Ba & 4Ba^2 & -6Ba & 2Ba^2 \\ -12B & -6Ba & 12B & -6Ba \\ 6Ba & 2Ba^2 & -6Ba & 4Ba^2 \end{bmatrix}, \quad B = EJ/a^3 \qquad (5)$$

where, m_r, a, E and J stand for the mass per unit length, length, Young's modulus and moment of inertia for the cross sections, respectively. The Hermite interpolation function is used as the shape function of the beam elements.

Based on the Hamilton's principle, the detailed derivation of the mass, stiffness and damping matrices of the turnout system is presented [14]. Finally, the dynamic equation of turnouts is established as shown in Equation (1).

Modal track model representation (Chalmers)

This track model entry concerns a modal representation of the track using modal damping. The track model has been implemented in Simpack 2021.2 using its linear flextrack capability. The use of a modal representation with modal damping means that the track model equations in Equation (1) are approximated by N decoupled differential equations on the form in Equation (6) [9].

$$\ddot{\rho}_r + 2\omega_r \zeta_r \dot{\rho}_r + \omega_r^2 \rho_r = \frac{f_r}{M_r}, \quad r = 1, 2, \ldots, N \qquad (6)$$

where ρ_r is the modal coordinate, ω_r the eigenfrequency, ζ_r the modal damping ratio, M_r is the modal mass and f_r the applied force for mode r. In analogy with a single degree of freedom system, a ζ_r value of one corresponds to critical damping for mode r. To go from Equation (1) to (6), the eigenmodes ($\boldsymbol{\varphi}_r$) and frequencies (ω_r) of the system are computed from the eigenvalue problem formulated from the undamped version of (1) according to Equation (7)

$$(\boldsymbol{K} - \omega^2 \boldsymbol{M})\boldsymbol{\varphi} = 0 \qquad (7)$$

The modal masses are then computed according to Equation (8)

$$M_r = \boldsymbol{\varphi}_r^T \boldsymbol{M} \boldsymbol{\varphi}_r, \quad r = 1, 2, \ldots, N \qquad (8)$$

The displacement and force relations between the representations is obtained via the coordinate transformations in Equation (9)

$$\boldsymbol{u} = \sum_{r=1}^{N} \boldsymbol{\varphi}_r \rho_r, \quad \boldsymbol{f} = \sum_{r=1}^{N} \boldsymbol{\varphi}_r f_r \qquad (9)$$

Equation (6) constitutes a direct equivalent to (1) if N is equal to the number of degrees of freedom in (1) and if the damping matrix $\boldsymbol{C}$ represents proportional (Rayleigh) damping such that it can be written as a scaled superposition of the mass and stiffness matrixes [9]. In this track model case, it will not be an exact representation of the FE model properties as (a) only a subset of the modes are selected to represent the track properties for improved numerical efficiency in the frequency range of interest and (b) the damping matrix in the FE model represents non-proportional damping. Solving for the undamped modes and adding modal damping afterwards (which corresponds to proportional damping) is therefore a simplification [29]. To more accurately represent (1) with a modal formulation, complex modes accounting for the non-proportional damping would have to be computed, but this is not supported in Simpack linear flextrack at the time of writing. To implement a track structure with non-proportional damping in Simpack, the non-linear flextrack option would need to be employed. Here the linear flextrack option was chosen for its comparatively lower computational effort and ease of modelling.

To generate the modal track model from the common FE model the following steps were performed in software in analogy with the steps outlined above.

- A 25-m plain line track extension was added in front of the turnout to allow for the initialisation of simulations with the vehicle outside of the main turnout structure.
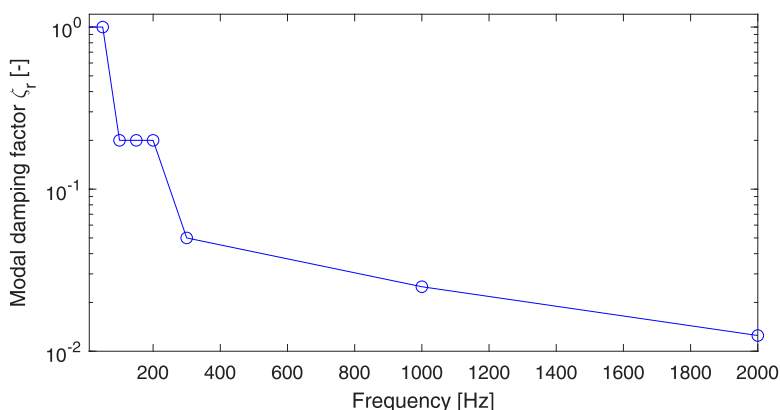
Figure 4. Modal damping factor as a function of frequency. Note logarithmic scale on the vertical axis.

- A modal analysis was performed in Abaqus using the base FE model to extract the undamped modes up to 2 kHz.
- A Simpack flexbody (.fbi file) was created from the modal results.
- A track body in Simpack of the type linear flextrack was created using the flexbody file
- The modal damping ratios ζ_r were defined as a function of frequency.

The cut-off frequency of 2 kHz is chosen based on the frequency range of interest as discussed in the description of the common FE-model. The influence of the cut-off frequency on the dynamic wheel–rail interaction at the crossing transition is further investigated at the end of the results section and it is shown that convergence in results is achieved at a cut-off of 750 Hz. The chosen frequency range should therefore be sufficient to represent the behaviour of the common FE model with a modal superposition approach.

For this track model there are 3625 modes up to 2 kHz. As there are 21,740 active dofs in the FE model (common FE model and track extension), this is a significant reduction in model size. The modal damping was adjusted to get acceptable agreement in track receptance response at two reference nodes between the modal representation of the track in Simpack and the corresponding results from the FE model. The modal damping ratio as a function of frequency is presented in Figure 4. The modal damping starts at $\zeta = 1$ (critical damping) up to 50 Hz and ends at $\zeta = 0.0125$ at 2 kHz. The first eigenfrequency is at 35 Hz. The high damping at low frequencies is motivated by the corresponding high damping of the reference model at low frequencies.
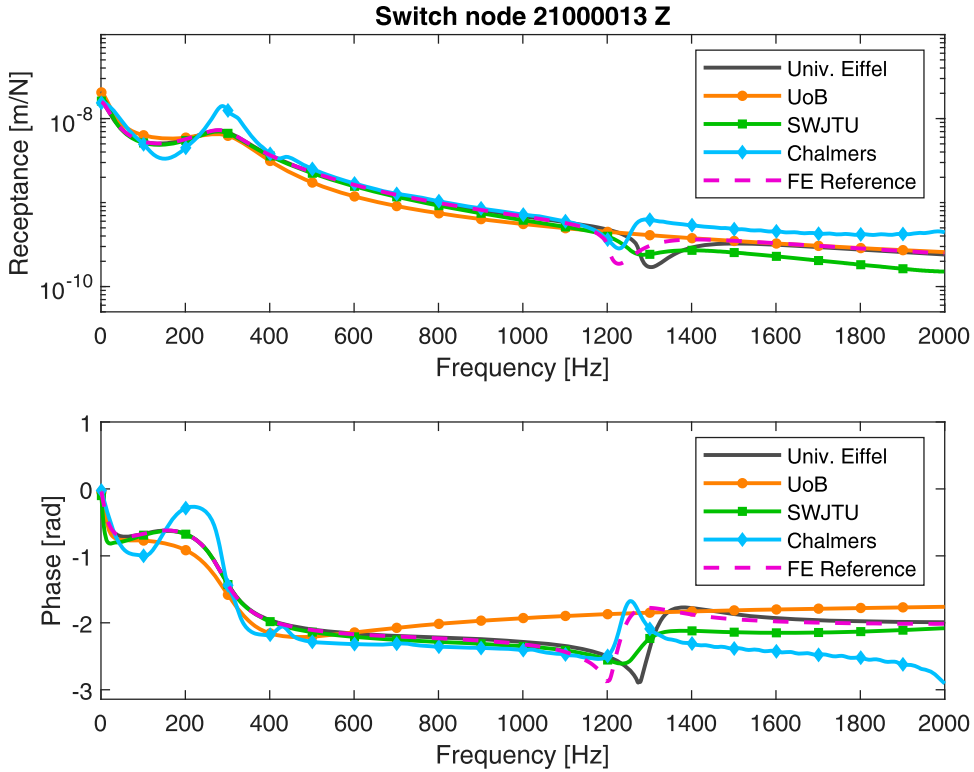
Comparison of track model behaviour in the frequency domain

The difference in track model behaviour between participants and modelling techniques is demonstrated by comparing the receptance at two representative nodes in the switch panel and at the crossing as listed in Table 2. The vertical receptances (amplitude and phase) for these nodes are plotted in Figures 5 and 6. The results include a reference result for the common track model computed directly in Abaqus. Several observations can be made

- The co-running model (UoB) does not capture the pinned-pinned frequency at 1200 Hz and has overall a smoother and more regular behaviour due to the lower number of dofs.

Table 2. Load nodes for receptance calculations.

Node	Load directions
Crossing node (25000079), located in the middle of the crossing rail	Lateral (Y) and vertical (Z). Vertical results presented.
Switch node (21000013), located on the straight stock rail 7.5 m from switch entry	Lateral (Y) and vertical (Z). Vertical results presented.

Figure 5. Receptance amplitude and phase at Switch node 21000013 in the vertical (z) direction.

- There is a slight difference in the location of the pinned-pinned frequency among the structural track models. This indicates a difference in beam element dynamic stiffness stemming from the beam element formulation or discretisation.
- The mode superposition approach with modal damping (Chalmers) demonstrates a shift in the low-frequency resonance peaks compared to the reference model. This appears to be due to the high non-proportional damping in the reference model. It was verified that a closer match could be obtained for lower levels of damping in the reference model.
- The FE models (Univ. Eiffel & SWJTU) show the closest agreement with the reference model.
- The agreement was found to be similar in the lateral direction but is not presented here.

This comparison naturally does not account for the differences that could appear in time-domain simulations due to the moving nature of the wheel–rail contact load. It has
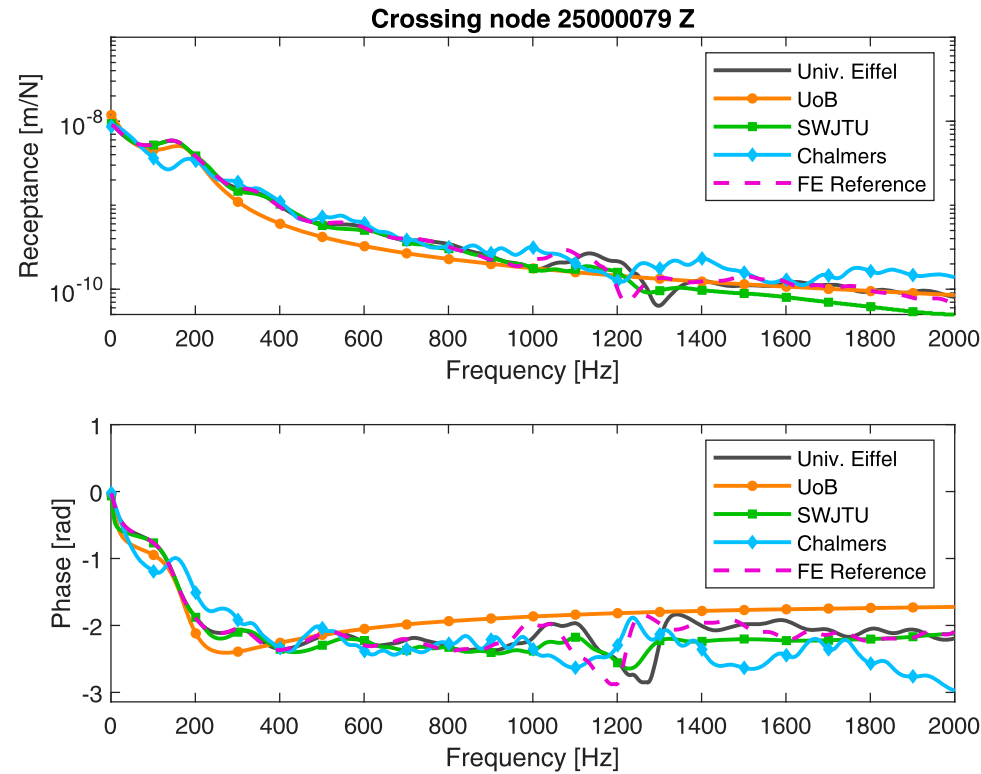
Crossing node 25000079 Z

Figure 6. Receptance amplitude and phase at Crossing node 25000079 in the vertical (z) direction.

however been demonstrated in [5] for a discretely supported rail that the influence on the receptance properties for realistic vehicle speeds is very small but around the pin-pin mode. The track model in this study is more comprehensive in comparison with more modes at lower frequencies and more inertia that could cause a greater speed dependence, but the effect is expected to be minor. The possible influence of speed dependence in track
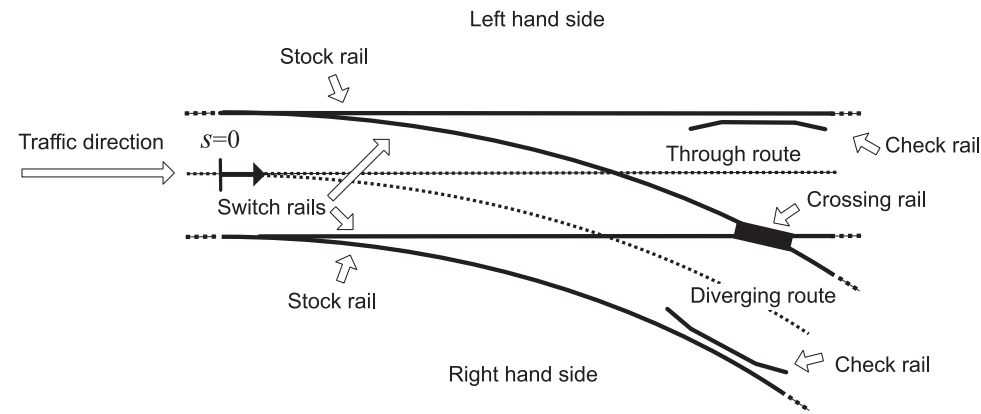

Figure 7. Turnout layout plan with traffic routes and rail body legends.

properties will also be accounted for implicitly in the next chapter with results from time-domain simulations.

Comparison of track model behaviour in the time domain

The different track formulations are compared in the time domain by simulating dynamic vehicle-track interaction in the facing move of the through and diverging routes of the turnout. The simulation cases correspond to those of the S&C benchmark for the 60E1-760-1:15 turnout [2]. The separate simulation runs for the switch and crossing panels used in the benchmark are joined into single simulations covering the full turnout given that the full turnout structure is considered here. The S&C benchmark uses a co-running track model with different properties for the switch and crossing panel simulations. Apart from the track model formulation, the simulation set-up used by all participants corresponds to those reported in the S&C Benchmark method statements [1]. Full details on the rail geometry implementation, wheel–rail contact modelling, time-domain integration method etc are given there.

The simulated traffic direction and the traffic routes are illustrated in Figure 7. The figure also includes the nomenclature for the different rails in the turnout assembly. As in the S&C benchmark, traffic is represented by the Manchester Benchmarks [30] passenger vehicle and the speed is 160 km/h in the through route and 80 km/h in the diverging route.

The change in track model formulation from co-running to a structural representation in the form of a FE or modal superposition model require solutions for the positioning of
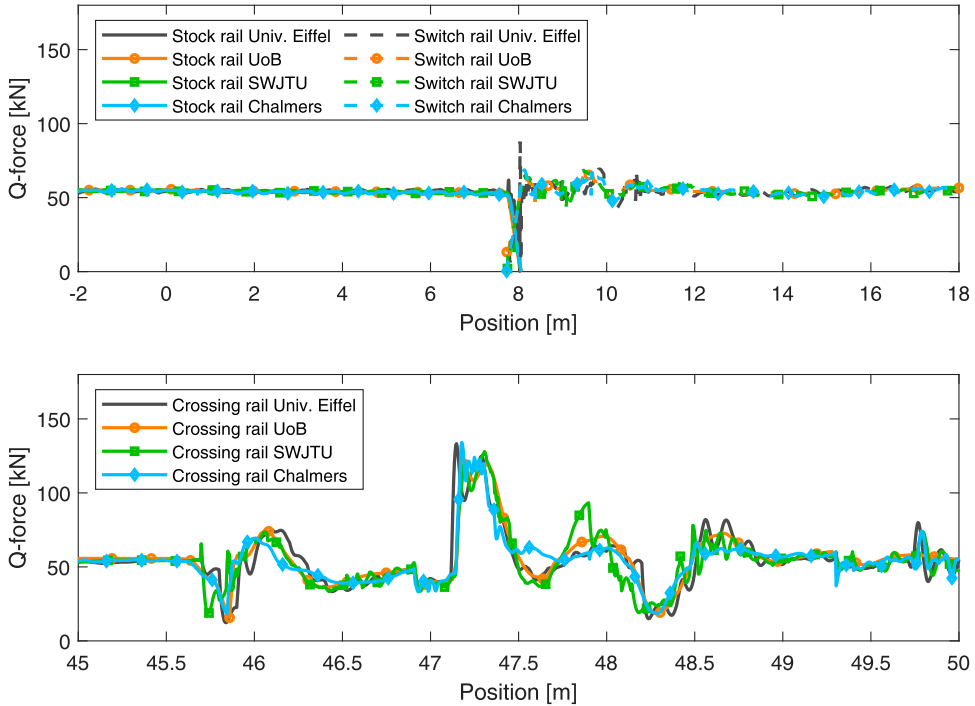

Figure 8. Q forces for leading wheelset as a function of position. Stock rail to switch rail transition (top) and over the crossing transition (bottom).

the rail profile coordinate system and mapping of the wheel–rail contact forces onto the nodes of the track model. In all of the present software, the rail profiles are positioned in the curvilinear coordinate system of the track according to a gauge and track irregularity definition and there is one rail coordinate system that follow each wheel along the track with a corresponding longitudinal position. This means that there will be a smooth trajectory of the rail profile also in the diverging route even if the rail is curved and described with a set of discrete nodes.

To couple the forces, torques and displacements at the wheel–rail interface to the track model and allow for the rail profile to displace relative to its nominal position due to track deformation, a mapping procedure is required. Both VOCO and SDITT uses Hermitian cubic shape functions to distribute the forces and torques from the rail profile onto the adjacent rail nodes along the track. The track displacements are also coupled to the rail node displacements via Hermitian shape functions. The lever arms for the torques introduced on the nodes from the offset of the wheel–rail contact forces are found by accounting for the offsets between the rail profile reference marker and the nodes. In the current investigations, the rail roll is not accounted for which means that the influence of any roll torque on the rail will not be visible. The details of the VOCO and SDITT approaches can be found in [25] and [14], respectively. In Simpack, a spline based interpolation technique is used to map forces and displacements between the rail profile and the track model nodes in the simulations [31].
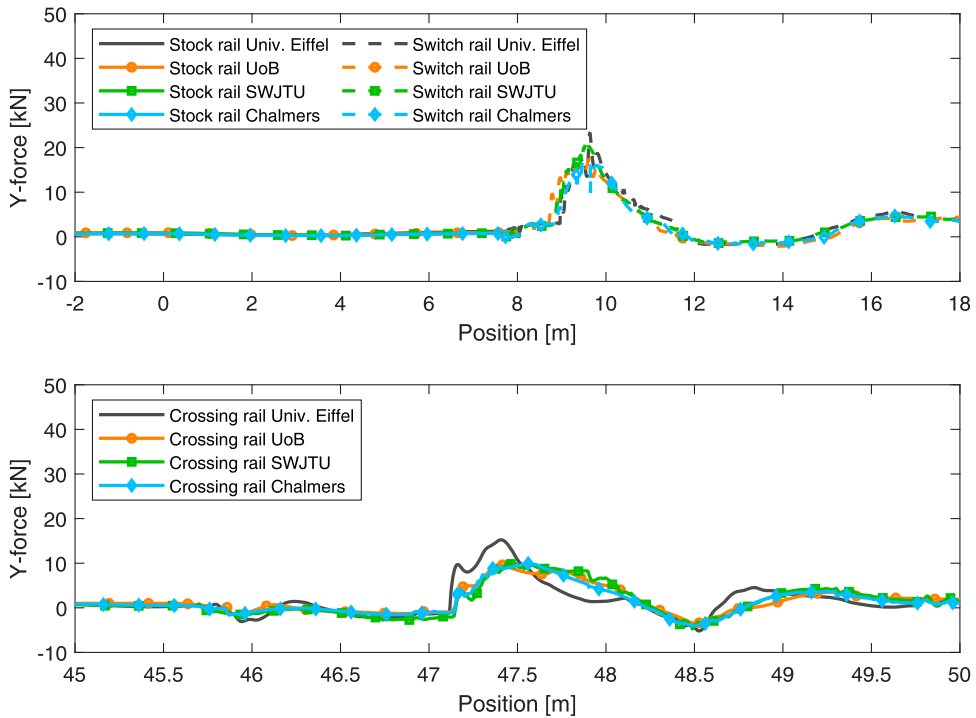

Figure 9. Y-forces for leading wheelset as a function of position. Stock rail to switch rail transition (top) and over the crossing transition (bottom). Lateral forces are positive on rail in the direction away from the track centreline.

Results through route

In the through route, the vertical dynamic excitation of interest can be found at the transitions from stock rail to switch rail and at the crossing. The resulting vertical wheel–rail contact force Q for the right-hand side wheel is presented in Figure 8. Due to the shallow kink in the vertical wheel trajectory at the switch transition, the magnitude of the dynamic excitation is low and the observable difference between the models low. At the crossing transition the variability is somewhat larger, but also here the overall agreement is good. The co-running track model (UoB) displays the least high frequency oscillations, followed by the modal superposition model (Chalmers). All models capture the P_1 and P_2 components of the impact load [23] on the crossing just after 47 m. The lateral Y-forces for the same wheel are shown in Figure 9. The force magnitudes are low and the agreement between the models good. The dynamic force magnitudes for the left wheel, which is running on a constant nominal 60E1 rail, are low and not presented here.

Figure 10 presents the vertical rail displacements under the right-hand side wheel (the forces of Figure 8). Overall, the agreement is good, but the co-running track model (UoB) deviates in two aspects in the switch panel. First, as both the switch rail and the stock rail bodies are present on the track mass throughout the simulation, the switch rail has a vertical rail displacement also before the actual switch rail is present along the track. In contrast, the switch rail displacement for the stationary track models is void until the wheel has reached the tip of the switch rail. Second, the relative displacement amplitude between the switch and stock rails is smaller for the co-running track model.
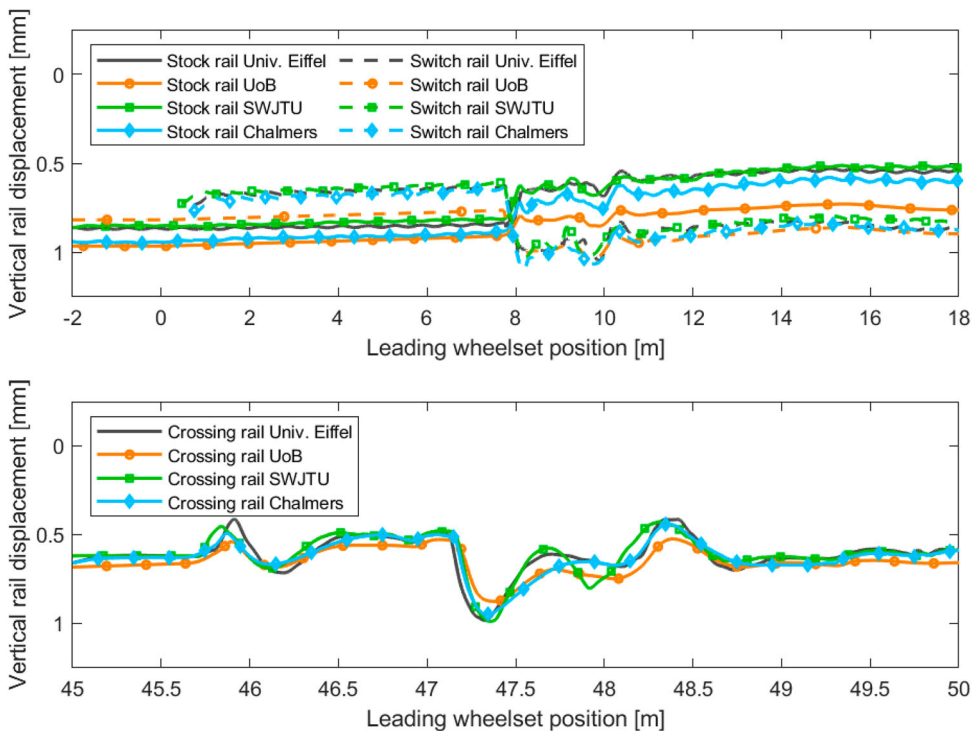

Figure 10. Vertical rail displacement under the leading axle for the stock rail to switch rail transition (top) and over the crossing transition (bottom).
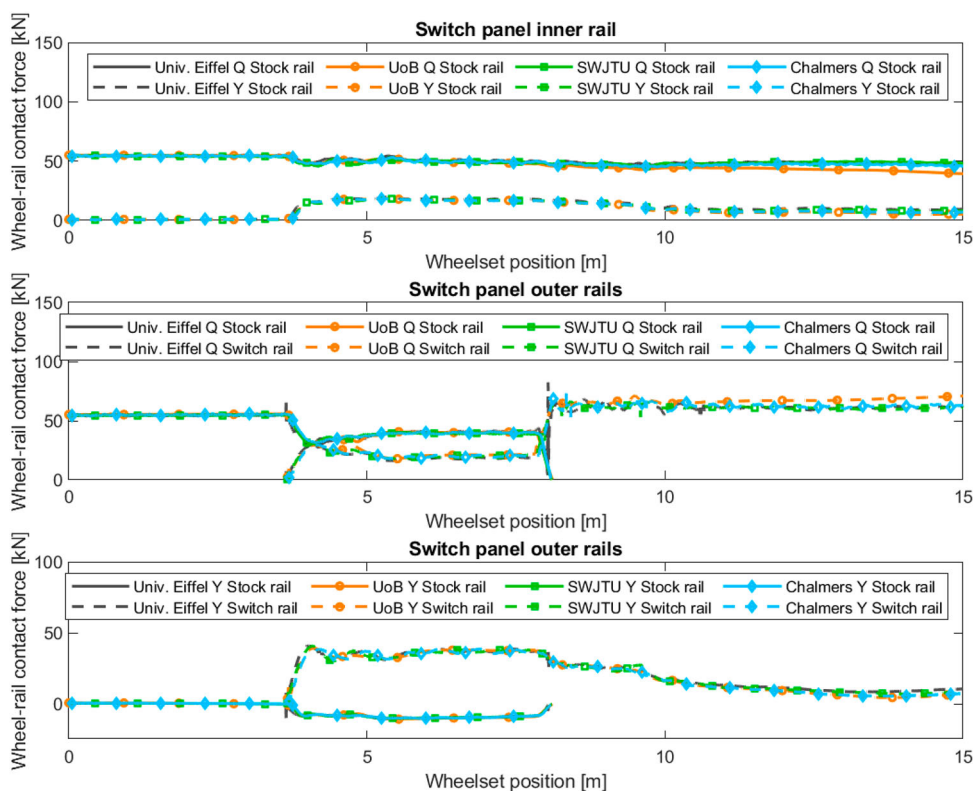
Figure 11. Wheel–rail contact forces for the leading wheelset as a function of position in the switch panel. Lateral forces positive on rail in the direction away from the track centreline.

Results diverging route

The results for the diverging route demonstrate a more complex behaviour than for the switch panel, and results are presented for both the outer (left-hand side) and inner (right-hand side) wheel of the leading wheelset. Due to the curve in the diverging route the outer wheel has an extended simultaneous contact with the switch and the stock rail. This can be observed in Figure 11 where the rails share the vertical load during this phase (middle figure, 4–8 m) and where the lateral forces are acting in opposite directions for the same period (bottom figure). The largest lateral force is carried by the switch rail which is in hard flange contact with the wheel. No significant discrepancies are found between the models.

The forces for the crossing panel are presented in Figure 12. The most notable loads concern the interaction with the check rail (top and middle figures) and the dynamic impact load at the crossing (bottom figure).

Vertical and lateral rail displacements for the diverging route are presented in Figures 13 and 14 for the switch and the crossing, respectively. The distinct features of the co-running track model (UoB) found for the through route are visible also here. The switch rail body is present from the start of the simulation and before it physically appears along the track, and the relative displacement magnitude between switch rail and stock rail is smaller.
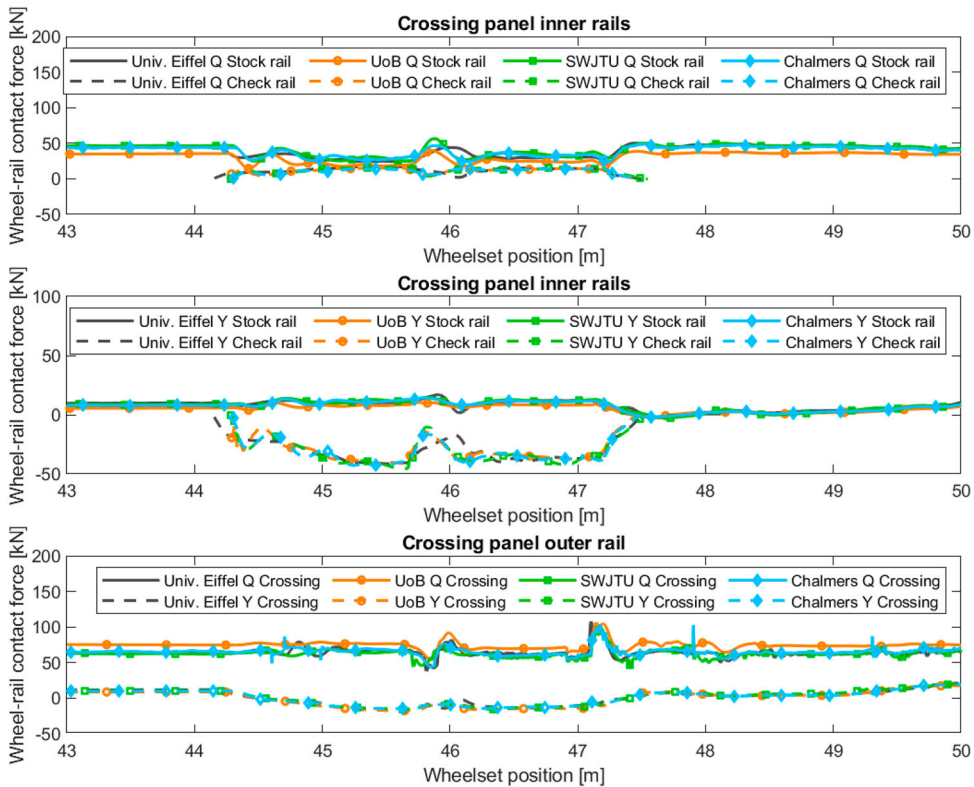
Figure 12. Wheel–rail contact forces for leading wheelset as a function of position in the crossing panel. Lateral forces positive on rail in the direction away from the track centreline.

Otherwise, the agreement between the models is good. As can be observed from the bottom of Figure 13, there is 1 mm of interpenetration between the switch rail and the stock rail. This interpenetration is made possible due to the simplified modelling of the fastening system in the switch panel with individual fastenings for both stock rail and switch rail. For the crossing panel results in Figure 14 the results for the co-running model are slightly offset from the structural track models.

The influence of track model frequency content

The influence of track model frequency content is here demonstrated by varying the frequency cut-off limit for the highest eigenmode in the modal superposition model. Figure 15 presents the vertical wheel–rail interaction force (Q) during the crossing transition for traffic in the through route for different eigenmode ranges. It can be observed that the force-time history is very similar for cut-off frequencies from 750 Hz and beyond while the response is much more oscillating for the cases with 100 and 250 Hz cut-off frequency. The track model has a significantly higher dynamic stiffness for the cases with 100 and 250 Hz cut-off frequency which can also be observed in the much greater force amplitudes for these cases. The greater force amplitudes are in correspondence with the higher dynamic stiffness for these track model configurations as illustrated in Figure 16. Given
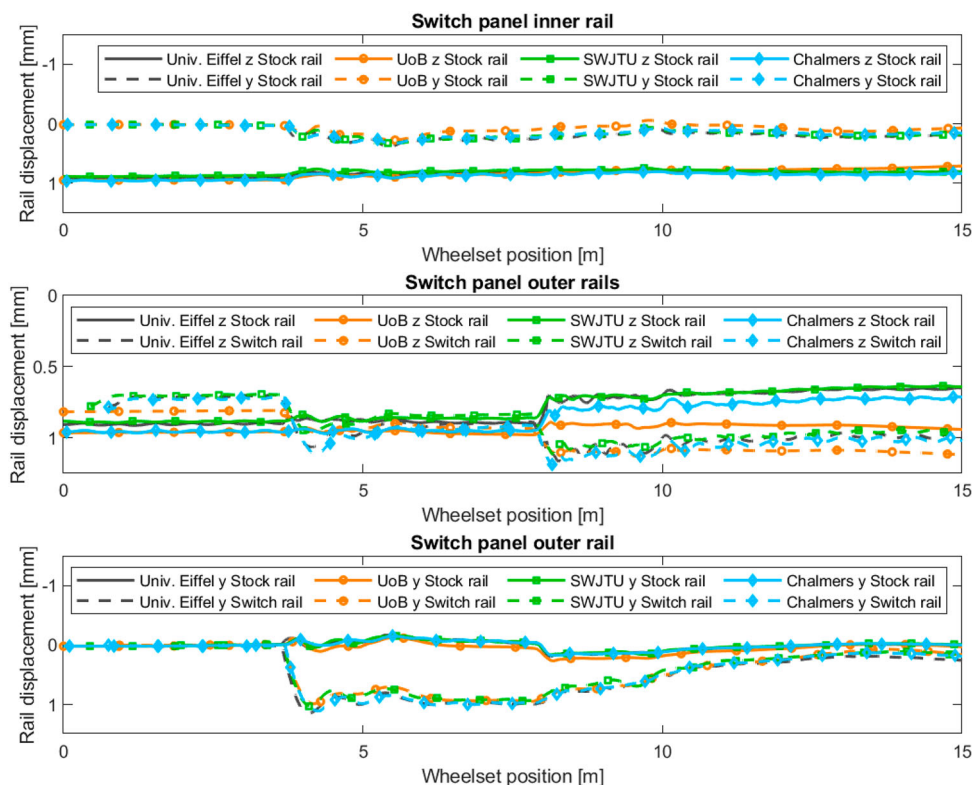
Figure 13. Rail displacements under the leading wheelset as a function of position in the switch panel. Lateral displacements positive away from track centreline.

the convergence in result beyond 750 Hz, these results also suggest that the pin-pin mode is of little significance for the modelling of the dynamic wheel–rail interaction at the crossing transition, at least for a nominal running surface of the crossing. The influence of the modal cut-off frequency was also studied in [10] for a similar track structure for 100, 250 and 500 Hz. Those results are qualitatively in agreement with the results presented here (higher impact load for a lower cut-off frequency), but with much smaller variability. As the properties vary between the models, these frequency ranges do not necessarily correspond to the same mode selection in the given frequency ranges and only the qualitative comparison can be made.

Comparison of computational effort

A comparison of the reported computational effort for the different models is presented in Table 3. The *relative computational effort per simulated second* quantity used for the comparison was computed by dividing the CPU time reported by the simulation software on each participant's computer with the simulated model time. The performance of each participant's computer varies somewhat as indicated by the table. The comparison should therefore only be taken as a qualitative indication of the computational effort taken by the different track modelling approaches and simulation software. The option of normalising
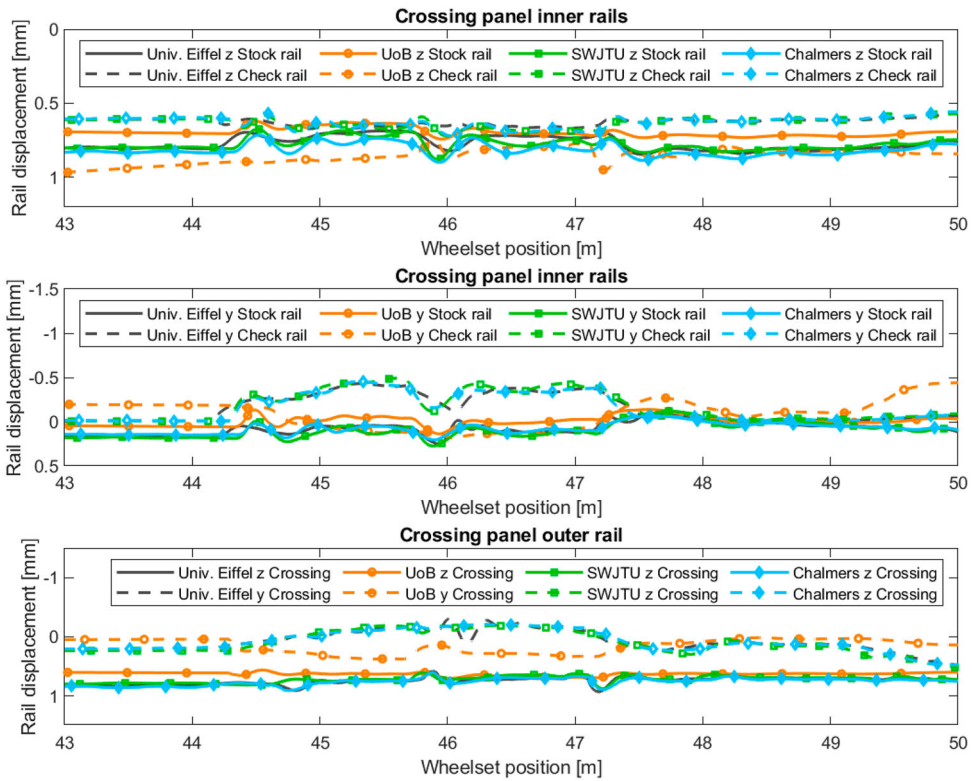
Figure 14. Rail displacements under the leading wheelset as a function of position in the crossing panel. Lateral displacements positive away from track centreline.
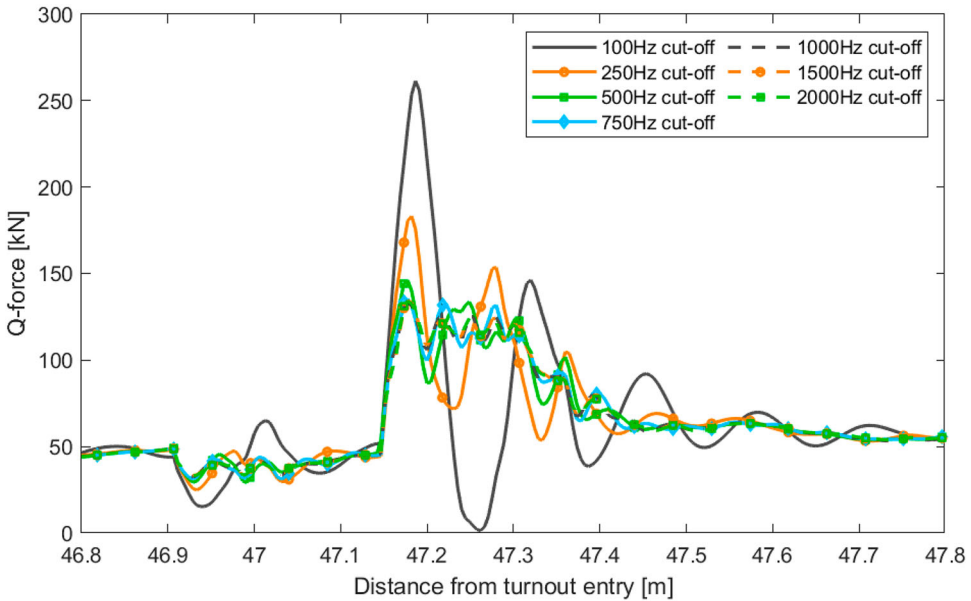

Figure 15. The vertical wheel–rail interaction force during the crossing transition for different eigen-mode frequency ranges in the modal superposition model.
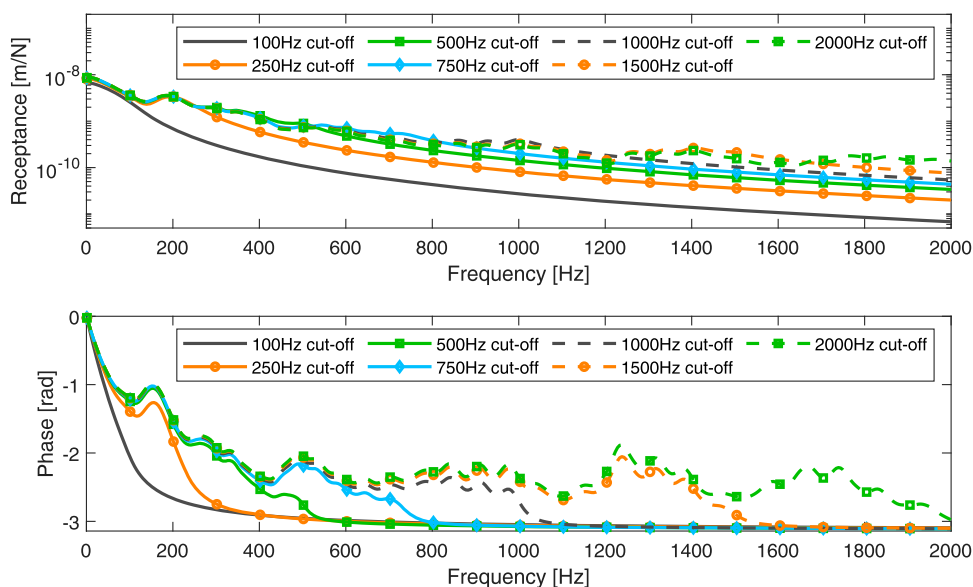
Figure 16. Vertical receptance and phase properties at the crossing transition (Node 25000079) for different eigenmode frequency ranges in the track model formulation.

Table 3. Computational effort for the different simulations in the through route.

Contribution	Computer specification (CPU and RAM)	Relative computational effort per simulated second in the model. X is in the order of 500 s.	#of dofs in the track model formulation
Univ. Eiffel	Dual processor Intel Xeon Gold 5222 CPU @ 3.80GHz RAM: 128 GB	CPU time: 60X	21740
UoB	Intel i7-7700 CPU @ 3.60GHz RAM: 64 GB	CPU time: X	19 per wheelset
SDITT	Intel i7-7700K CPU @ 4.20GHz RAM: 32 GB	CPU time: 17X	10687
Chalmers (2 kHz cut-off frequency)	Intel i5-7500 CPU @ 3.40GHz RAM: 16 GB	CPU time: 1.5X	3625

the CPU times to a common benchmark code between the computers was considered, but with this approach it would still be uncertain how representative this code would be for the present simulations. The ideal comparison of running the different track model configurations within the same software environment on the same computer is left for future work.

As expected, the simulation effort is significantly influenced by the number of degrees of freedom in the model, but there is no direct proportionality. Especially it can be noted that the relative simulation effort between the Chalmers and UoB approaches is small while the difference in the number of dofs for the track models is about a factor of 30. Though no full explanation for this can be provided within the scope of this paper, it is hypothesised that the time step is mainly determined by the very stiff wheel–rail contact which reduces the influence of a large number of dofs in the track model. It can be noted that a procedure has recently been proposed that can get similar results for co-simulation with a reduction of the computing time by a factor of 10 [32].

Table 4. Proposed advantages and disadvantages of each track model formulation.

	Advantages	Disadvantages
Co-running	• Low computational effort • Can provide an accurate track representation up to the pinned-pinned mode ($\sim$ 1 kHz) in frequency given sufficient model complexity.	• No physical interpretation of track response below the rail level • Requires tuning to target global track behaviour.
Modal Superpositon	• Low computational effort while allowing for evaluation of the full track response • Frequency range in track representation easily defined by user	• Requires a base FE track model for its generation • The approximation of normal modes and proportional damping is less accurate if the base model has high levels of non-proportional damping
Finite element in Co-simulation	• True representation of FE model behaviour • Allows for the utilisation of an existing FE model without further modification • Allows for full FE detail modelling capability available in FE software, for example contact non-linearities	• Computationally demanding
Finite element in MBS	• True representation of FE model behaviour • Easy to account for non-linearities (e.g. non-linear contact between the switch rail and stock rail in lateral direction)	• Computationally demanding

Conclusions

This study has found a good agreement in results between the different track model formulations for the studied output channels and the given linear FE model reference. The co-running track model captures less detail and exhibits less of the higher frequency behaviour found in the structural track models but captures the global wheel–rail interaction behaviour very well. The co-running track model does not capture the pinned-pinned frequency (around 1200 Hz in this model), but on the other hand the modal cut-off frequency convergence study demonstrated that modes above 750 Hz contribute little to the vertical dynamic impact load at the crossing transition for the modelling detail captured by the FE model and the nominal crossing geometry used in these investigations.

This study found a better agreement between co-running and structural track models compared to previous studies for S&C [10,16,17]. Contrasting the models and the methods in the different papers, this appears to be due to the increased complexity of co-running track model used in this study together with a tuning of the co-running track model to the base model in a wider frequency range.

Given that all the investigated models can provide good agreement for the prediction of dynamic wheel–rail interaction forces in S&C, the choice of model formulation for a prospective modeller will have to be determined by the intended application. If for example the structural response below the rail level is sought, the co-running track model cannot provide results with a direct physical interpretation as it consists of an equivalent system of bodies and bushings. If the modeller wishes to include non-linear track properties such as contact conditions, any of the full FE model approaches appear most suitable. Examples of

advantages and disadvantages for the different track models covered in this study are listed in Table 4. For an overview of the modelling detail required to capture different physical phenomena and damage modes in track modelling, see e.g. [5].

Acknowledgements

Disclosure statement

Funding

ORCID

Björn A. Pålsson http://orcid.org/0000-0002-2237-8560
Ramakrishnan Ambur http://orcid.org/0000-0003-0636-0894
Ping Wang http://orcid.org/0000-0002-2088-9279
Jou-Yi Shih http://orcid.org/0000-0002-7834-2305
Demeng Fan http://orcid.org/0000-0002-3681-7325
Jiayin Chen http://orcid.org/0000-0003-1118-977X

References

[1] Bezin Y, Pålsson BA, Kik W, et al. Multibody simulation benchmark for dynamic vehicle-track interaction in switches and crossings: results and method statements. Veh Syst Dyn. 2021. doi:10.1080/00423114.2021.1959038.
[2] Bezin Y, Pålsson BA. Multibody simulation benchmark for dynamic vehicle-track interaction in switches and crossings: modelling description and simulation tasks. Veh Syst Dyn. 2021. doi:10.1080/00423114.2021.1942079.
[3] Pålsson BA. Repository for 60E1 760 1:15 finite element turnout model. Chalmers University of Technology. 2021. Available from: https://doi.org/10.5878/6j4g-y180.
[4] Chaar N, Berg M. Simulation of vehicle-track interaction with flexible wheelsets, moving track models and field tests. Veh Syst Dyn. 2006;44:921–931.
[5] Knothe KL, Grassie SL. Modeling of railway track and vehicle track interaction at high-frequencies. Veh Syst Dyn. 1993;22(3–4):209–262.
[6] Costa JN, Antunes P, Magalhaes H, et al. A novel methodology to automatically include general track flexibility in railway vehicle dynamic analyses. P I Mech Eng F J Rai. 2021 Apr;235(4):478–493.

[7] Alfi S, Bruni S. Mathematical modelling of train-turnout interaction. Veh Syst Dyn. 2009;47(5):551–574.

[8] Antunes P, Magalhaes H, Ambrosio J, et al. A co-simulation approach to the wheel-rail contact with flexible railway track. Multibody Syst Dyn. 2019 Feb;45(2):245–272.

[9] Craig RR, Kurdila A, Craig RR. Fundamentals of structural dynamics. 2nd ed. Hoboken (NJ): John Wiley; 2006.

[10] Kassa E, Nielsen JCO. Dynamic train-turnout interaction in an extended frequency range using a detailed model of track dynamics. J Sound Vib. 2009 Mar 6;320(4–5):893–914.

[11] Wang P. Design of high-speed railway turnouts: theory and applications. London: Academic Press; 2015.

[12] Sebès M, Bezin Y. Considering the interaction of switch and stock rails in modelling vehicle-track interaction in a switch panel diverging route. Veh Syst Dyn. 2021. doi:10.1080/00423114.2021.1947510.

[13] Shu X, Schreiber P, Wilson N, et al. Modeling stock and switch rail interaction. Submitted to VSD. 2020.

[14] Chen JY, Chen R, Xu JM, et al. Simulation of vehicle-turnout coupled dynamics considering the flexibility of wheelsets and turnouts. Submitted to VSD. 2021.

[15] Iwnicki S, editor. Handbook of railway vehicle dynamics. Boca Raton (FL): CRC Taylor & Francis; 2006.

[16] Bruni S, Anastasopoulos I, Alfi S, et al. Train-induced vibrations on urban metro and tram turnouts. J Transp Eng ASCE. 2009 Jul;135(7):397–405.

[17] Jorge P, Bezin Y, Grossoni I, et al. Modelling track flexibility in turnouts using MBS approach. In: Klomp M, Bruzelius F, Nielsen J, et al., editors. Advances in dynamics of vehicles on roads and tracks. IAVSD 2019. Cham: Springer; 2020. (Lecture Notes in Mechanical Engineering). doi:10.1007/978-3-030-38077-9_42.

[18] Wan C, Markine VL, Shevtsov IY. Improvement of vehicle-turnout interaction by optimising the shape of crossing nose. Veh Syst Dyn. 2014 Nov 2;52(11):1517–1540.

[19] Di Gialleonardo E, Braghin F, Bruni S. The influence of track modelling options on the simulation of rail vehicle dynamics. J Sound Vib. 2012 Sep 10;331(19):4246–4258.

[20] Shih JY, Kostovasilis D, Bezin Y, et al. Modelling options for ballast track dynamics. The 24th International Congress on Sound and Vibrations; 23–27 July; London, UK; 2017.

[21] Yang J, Thompson DJ, Takano Y. Characterizing wheel flat impact noise with an efficient time domain model. Notes Numer Fluid Me. 2015;126:109–116.

[22] Palsson BA, Nielsen JCO. Dynamic vehicle-track interaction in switches and crossings and the influence of rail pad stiffness – field measurements and validation of a simulation model. Veh Syst Dyn. 2015 Jun 3;53(6):734–755.

[23] Jenkins HH, Stephenson JE, Clayton GA, et al. The effect of track and vehicle parameters on wheel/rail vertical dynamic forces. Railw Eng J. 1974;3(1):2–16.

[24] Shih JY, Ambur R, Dixon R. Developing a detailed multi-body dynamic model of a turnout based on its finite element model. Veh Syst Dyn. 2020. doi:10.1080/00423114.2021.1981952.

[25] Sebes M, Chollet H, Monteiro E, et al. Adaptation of the semi-Hertzian method to wheel/rail contact in turnouts. Dynamics of vehicles on roads and tracks: proceedings of the 24th symposium of the international association for vehicle system dynamics (IAVSD 2015), Graz, Austria, 17– 21 August 2015 (1st ed.). CRC Press; 2016. p. 1367–1376.

[26] Bezin Y, Iwnicki SD, Cavalletti M, et al. An investigation of sleeper voids using a flexible track model integrated with railway multi-body dynamics. P I Mech Eng F J Rai. 2009 Nov;223(6):597–607.

[27] Sebès M, Fan D, Qazi A, et al. VOCO statement of methods S&C Benchmark. 2020. doi:10.34696/s60x-ay18.

[28] Ansys. Academic research mechanical, release 20.1, help system, mechanical APDL theory reference. 2021.

[29] He J, Fu Z-F. Modal analysis. Oxford: Butterworth-Heinemann; 2001.

[30] Iwnicki S. Manchester benchmarks for rail vehicle simulation. Veh Syst Dyn. 1998 Sep;30(3–4):295–313.

[31] Simpack. Simpack documentation v. 2021.2, Dassault Systemes, 2021. https://www.3ds.com/products-services/simulia/products/simpack/.

[32] Fan D, Sebès M, Qazi A, et al. A fast co-simulation approach to vehicle/track interaction with finite element models of S&C. Accepted to IAVSD2021; 2021.

[33] In2Track. Deliverable 2.2, enhanced S&C whole system analysis, design and virtual validation (final), Chapter 3. 2019.

[34] Pålsson BA. A parameterized turnout model for simulation of dynamic vehicle-turnout interaction with an application to crossing geometry assessment. In: Klomp M, Bruzelius F, Nielsen J, et al., editors. Advances in dynamics of vehicles on roads and tracks. IAVSD 2019. Cham: Springer; 2020. (Lecture Notes in Mechanical Engineering). doi:10.1007/978-3-030-38077-9_41.

[35] Nielsen JCO. High-frequency vertical wheel-rail contact forces – validation of a prediction model by field testing. Wear. 2008 Oct 30;265(9–10):1465–1471.

[36] Grossoni I, Bezin Y, Neves S. Optimisation of support stiffness at railway crossings. Veh Syst Dyn. 2018;56(7):1072–1096.

[37] Chaar N. Wheelset structural flexibility and track flexibility in vehicle-track dynamic interaction [PhD]. Stockholm: Royal Institute of Technology (KTH); 2007.

[38] Andersson E, Berg M, Stichel S, et al. Rail vehicle dynamics. Stockholm: Railway Group KTH, Kungliga Tekniska högskolan; 2014.

[39] CEN. EN 13674-2:2006: E. Brussels: CEN.

Appendix. Description of common FE model

The investigations in this paper use a finite element model of a 60E1-760-1:15 turnout as a common base. The model has been generated using a turnout model script developed within the Shift2Rail research program and the projects In2Track [33] and In2Track2 [34]. The purpose of this script is to allow for the creation of turnout models of different sizes and properties. The models are by necessity rather generic and are intended to be representative but not exact representations of any specific turnout design. The script takes the following parameters as input

- Turnout radius and sleeper spacing
- Mass and area moment of inertia for rails and sleepers
- Stiffness and damping properties for rail pads, ballast, and check rail fastenings
- Finite element discretisation in terms of typical element lengths and nodal degrees of freedom

The script generates models of standard right-hand turnouts with constant curvature and a tangential entry into the switch. The models have two structural layers where rails and sleepers are modelled using beams and rail fastenings and sleeper to ballast properties are modelled using linear bushing elements. The resulting layouts for the switch and crossing panels for the 60E1-760-1:15 including rail and sleeper bodies are illustrated in Figure A1. For modelling simplicity, the check rail bodies overlap with the stock rails in the crossing panel. The body properties are listed in Table A1 and FEM discretisation details are given in Table A2. All bodies have constant properties throughout their length but for the switch rails. These are tapered up to about 10.5 m into the switch and then continue with constant cross sections up to 21 m into the turnout where they transition to standard 60E1 rails.

The bushing connection topology with discrete supports between rails and sleepers and sleepers and ground are illustrated in Figure A3. Each bushing element has stiffness and damping in multiple directions. The same rail pad properties are used throughout but for the check rail that has a higher lateral stiffness. The sleeper to ballast properties are given per metre sleeper length, and the lumped properties for each bushing element in the model is computed by accounting for the sleeper-ballast contact length represented by each single element.

The bushing properties are given in Table A1. The vertical rail pad properties are taken from [35]. The rotational rail pad properties have been computed from the vertical stiffness by assuming a
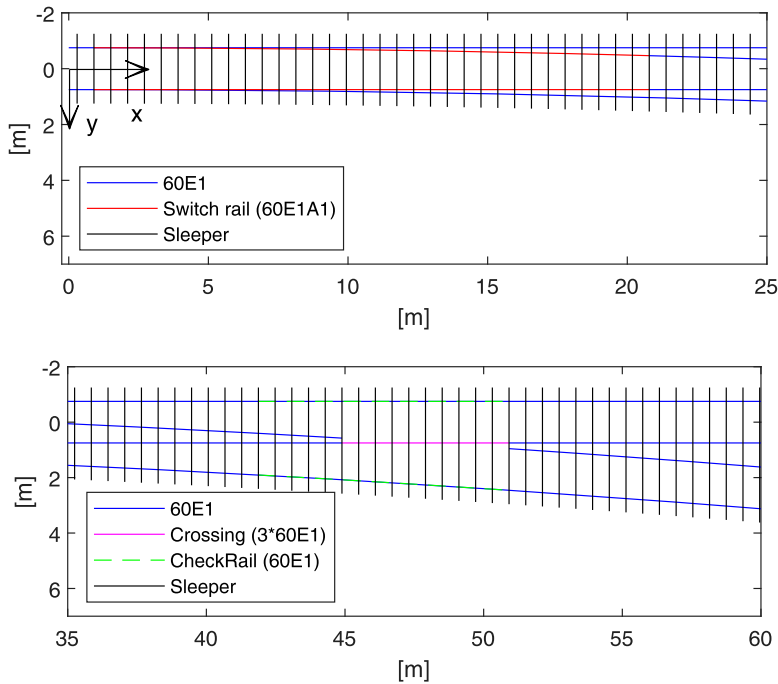
Figure A1. Top view of switch panel (top) and crossing panel (bottom) with rail and sleeper body designations and reference coordinate system. The *z*-direction is positive downwards (not shown).

Table A1. Rail and sleeper bodies and their properties. Area moment of inertias (*I*) are given w.r.t vertical (1) and horizontal (2) axes in a plane transversal to the elongation of each body.

Rail type	Properties
60E1	$M = 60$ kg/m (mass per metre rail)
	$I_{11} = 5.1\text{e-}6$ m^4
	$I_{22} = 30.3\text{e-}6$ m^4
Crossing	M, I_{11} and I_{22} have values three times those of 60E1
Check rail	Same as 60E1
Switch rail (60E1A1 [39])	$M = 73$ kg/m (mass per metre rail)
	$I_{11} = 7.4\text{e-}6$ m^4
	$I_{22} = 17.3\text{e-}6$ m^4
	The tapered section has varying properties according to Figure A2.
Sleeper	$M = 131$ kg/m (mass per metre sleeper)
	$I_{11} = 278\text{e-}6$ m^4
	$I_{22} = 224\text{e-}6$ m^4

Table A2. Track model discretisation properties.

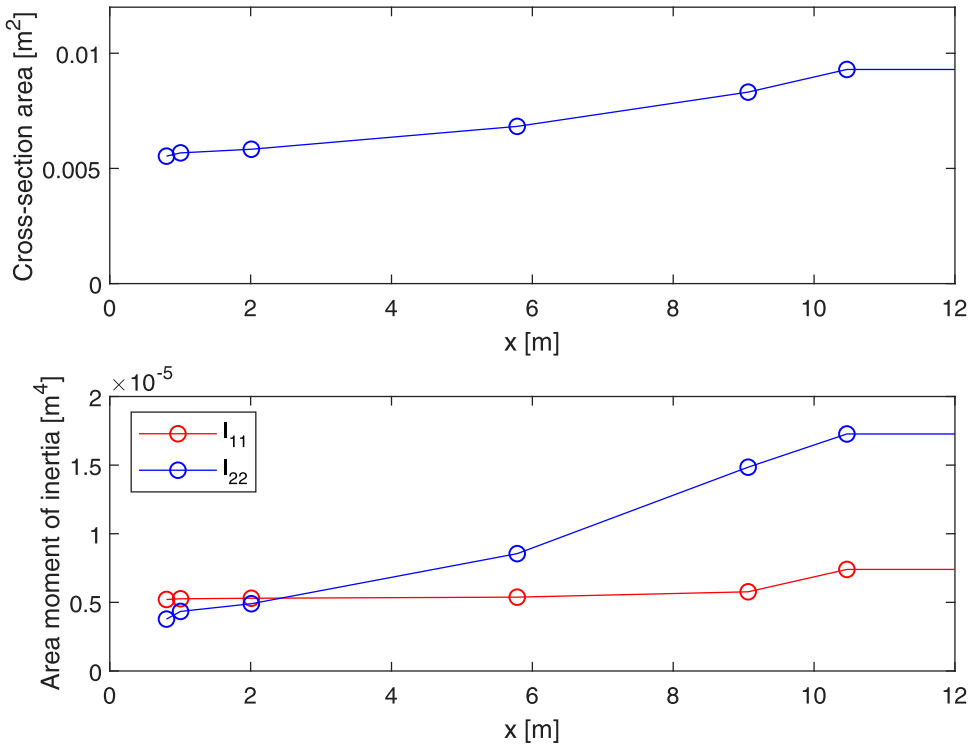| **Rails**	
Typical element length	0.15 m, four beam elements per sleeper span
Constrained nodal degrees of freedom	x translation and x rotation
Sleepers	
Typical element length	0.125 m
Constrained nodal degrees of freedom	x translation, y and z rotation
Other	
Element type for all bodies	Abaqus element formulation B31 (Linear Timoshenko). The default shear factor of one is used.

Figure A2. Cross-section properties for switch rail as a function of track position. Circles indicate locations for cross-section reference data.
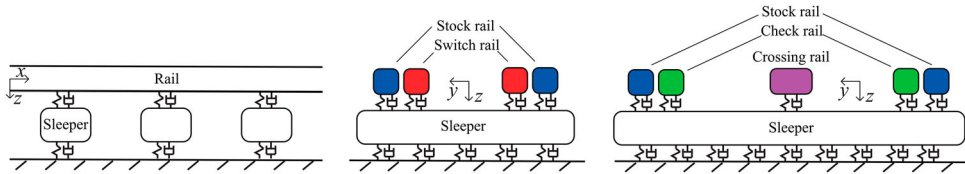

Figure A3. Track model topology. Longitudinal cross-section (left) and cross sections in switch panel (middle) and crossing panel (right).

square rail pad with sides 0.1 m. The ballast stiffness corresponds to that used in [36] and is somewhat lower than typically reported values [5]. The ballast damping has been adjusted to reach a qualitative agreement with the high damping at low excitation frequencies observed in track stiffness measurements in the range 0–50 Hz in [37] and at 10 and 20 Hz in [22,37]. The lateral stiffness properties are assumed but have been informed by the ratios between vertical and lateral track stiffness found in [37,38].

As can be observed from the description the model includes several simplifications. Notable modelling assumptions that have been introduced to simplify modelling and allow for a fully linear track model are

- Switch rails are connected to the sleepers only with individual pads. No base plates or contact conditions are introduced.
- The structural representation of the check rails overlap with the stock rails.

Table A3. Track model bushing properties. The properties in rows one to eight are for discrete elements while the ballast properties in rows nine to twelve are given per metre in the lengthwise direction of the sleeper.

Parameter	Value
Rail pad stiffness vertical	120 MN/m
Rail pad stiffness lateral	25 MN/m.
Rail pad damping vertical	25 kNs/m
Rail pad damping lateral	10 kNs/m
Check rail mounting stiffness vertical	120 MN/m
Check rail mounting stiffness lateral	120 MN/m
Rotational stiffness for all rail to sleeper connections in all directions	100 kNm/rad
Rotational damping for all rail to sleeper connections in all directions	20 Nms/rad
Ballast stiffness vertical. Corresponds to a bed modulus of $\sim$ 67 MN/m^3 and a sleeper base width of 0.3 m.	20 MN/m/m
Ballast stiffness lateral	10 MN/m/m
Ballast damping vertical	200 kNs/m/m
Ballast damping lateral	100 kNs/m/m

- The crossing beam elements are oriented according to traffic in the through route. Rearrangement of the model or interpolation of the rail profile reference marker is therefore required for the simulation of traffic in the diverging route.
- Both switch rails are modelled in their closed position to allow for simulation of traffic in both the through and the diverging route depending on contact definition.

The model and a corresponding Matlab script that allow for the modification of bushing stiffnesses and nodal constraints are available for download under a CC BY open source license [3]. This article must be referenced if this model is used for work that results in a publication.